Clinical Cancer Research

# Recurrent *TRIO* Fusion in Nontranslocation–Related Sarcomas

Lucile Delespaul[1,2], Tom Lesluyes[1,2], Gaëlle Pérot[1,3], Céline Brulard[1], Lydia Lartigue[1,2], Jessica Baud[1,2], Pauline Lagarde[1], Sophie Le Guellec[4], Agnès Neuville[1,3], Philippe Terrier[5], Dominique Vince-Ranchère[6], Susanne Schmidt[7], Anne Debant[7], Jean-Michel Coindre[1,2,3], and Frédéric Chibon[1,3]

## Abstract

**Purpose:** Despite various differences, nontranslocation-related sarcomas (e.g., comprising undifferentiated pleomorphic sarcoma, leiomyosarcoma, myxofibrosarcoma) are unified by their complex genetics. Extensive analysis of the tumor genome using molecular cytogenetic approaches showed many chromosomal gains, losses, and translocations per cell. Genomic quantitative alterations and expression variations have been extensively studied by adapted high-throughput approaches, yet translocations still remained unscreened. We therefore analyzed 117 nontranslocation-related sarcomas by RNA sequencing to identify fusion genes.

**Experimental design:** We performed RNA sequencing and applied a bioinformatics pipeline dedicated to the detection of fusion transcripts. RT-PCR and Sanger sequencing were then applied to validate predictions and to search for recurrence and specificity.

**Results:** Among the 6,772 predicted fusion genes, 420 were in-frame. One recurrent rearrangement, consistently involving *TRIO* with various partners, was identified in 5.1% of cases. *TRIO* translocations are either intrachromosomal with *TERT* or interchromosomal with *LINC01504* or *ZNF558*. Our results suggest that all translocations led to a truncated TRIO protein either directly or indirectly by alternative splicing. *TRIO* rearrangement is associated with a modified transcriptomic program to immunity/inflammation, proliferation and migration, and an increase in proliferation.

**Conclusions:** *TRIO* fusions have been identified in four different sarcoma histotypes, likely meaning that they are not related to a primary oncogenic event but rather to a secondary one implicated in tumor progression. Moreover, they appear to be specific to nontranslocation-related sarcomas, as no such rearrangement was identified in sarcomas with simple genetics. More cases could lead to a significant association of these fusions to a specific clinical behavior. *Clin Cancer Res; 23(3); 857–67. ©2016 AACR.*



## Introduction

Sarcomas represent a heterogeneous group of rare tumors accounting for approximately 1% of adult cancers with more than 50 histologic subtypes. These tumors, derived from mesenchymal tissues (i.e., soft tissue, bone, or muscle), are classified on the basis of their line of differentiation, following the World Health Organization (WHO) recommendations (1). Along with this histologic heterogeneity, sarcoma genetics is also highly heterogeneous in terms of oncogene-specific driver alterations and whole-genome instability. Sarcomas can be classified into two groups depending on genome stability. One group consists of sarcomas with a relatively stable genome with specific oncogenic alterations (rare gains and losses involving mainly full chromosomes). Among these, gastrointestinal stromal tumors (GIST; *KIT* or *PDGFRA* mutations; ref. 2) and sarcomas with a specific translocation (e.g., Ewing sarcoma, synovial sarcoma, and alveolar rhabdomyosarcoma; refs. 3–5) represent 20% and 30% of sarcomas, respectively. The second group consists of nontranslocation-related sarcomas with higher chromosomal instabilities and pleomorphic histologic patterns. There is no specific genetic alteration described so far in those sarcomas. Nevertheless, we can distinguish well-differentiated and dedifferentiated liposarcoma (20% of sarcomas) with recurrent *MDM2* and *CDK4* amplification within a moderately rearranged profile (6, 7). The remaining 30% mainly comprise leiomyosarcoma, undifferentiated pleomorphic sarcoma, myxofibrosarcoma, pleomorphic liposarcoma, and pleomorphic rhabdomyosarcoma. Although their genomic instability has not been deciphered yet, some recurring genetic alterations have been identified in these tumors: the 13q14-21 region is frequently lost in leiomyosarcomas and undifferentiated pleomorphic sarcoma targeting *RB1* deletion/inactivation (8); the TP53 pathway is consistently inactivated, mainly by *TP53* deletions/mutations (9); and a gain of 5p region is also frequent and triggers *TRIO* amplification (10, 11). Extensive

[1]Inserm U916, Bergonié Cancer Institute, Bordeaux, France. [2]University of Bordeaux, Bordeaux, France. [3]Department of Pathology, Bergonié Cancer Institute, Bordeaux, France. [4]Department of Pathology, University Cancer institute Toulouse-Oncopole, Toulouse, France. [5]Department of Pathology, Gustave Roussy Institute, Villejuif, France. [6]Department of Pathology, Léon Bérard Center, Lyon, France. [7]Centre de Recherche en Biologie Cellulaire de Montpellier, CRBM, CNRS-UMR 5237, University of Montpellier, Montpellier, France.

**Note:** Supplementary data for this article are available at Clinical Cancer Research Online (http://clincancerres.aacrjournals.org/).

**Corresponding Author:** Frédéric Chibon, Institut Bergonié, 229 Cours de l'Argonne, Bordeaux 33000, France. Phone: 055-633-4443; Fax: 055-633-4438; E-mail: F.chibon@bordeaux.unicancer.fr

**doi:** 10.1158/1078-0432.CCR-16-0290

## Translational Relevance

Nontranslocation-related sarcoma is one of the most common and aggressive subtype of soft tissue sarcomas. Despite extensive quantitative and structural characterization of their genome and transcriptome, it remains the largest sarcoma group without any specific genetic alteration that can be targeted for therapy. Therefore, treatment is still based on surgery with wide margins. Previous high-throughput studies based on quantitative analysis failed to identify such specific alteration. We thus applied RNA sequencing on a large cohort of nontranslocation-related sarcomas from the French Sarcoma Group and identified recurrent, and so far specific, *TRIO* fusions with various partners. Fusion-positive tumors belong to four different histotypes, likely meaning that fusions are not related to a specific primary oncogenic event but rather to a secondary one implicated in tumor progression. Our data suggest that fusion triggers a modified transcriptomic and phenotypic program that could lead to an increase in cell proliferation.

analysis of the tumor genome by molecular cytogenetic approaches showed many breakpoints [array comparative genomic hybridization (aCGH)] and translocations per cell (chromosome painting; refs. 12, 13). Breakpoints located in coding regions are supposed to produce chimeric transcripts with potent oncogenic effects. It has been demonstrated that RNA sequencing (RNA-seq) is an efficient approach to identify fusion transcripts in tumors, particularly in sarcomas (14–16). Hence, we subjected 117 nontranslocation-related sarcomas to RNA-seq to identify fusion transcripts.

## Materials and Methods

### Ethics statement

The samples used in this study are part of the Biological Resources Center of Institut Bergonié (CRB-IB; Bordeaux, France). In accordance with the French Public Health Code (articles L. 1243-4 and R. 1243-61), the CRB-IB has received the agreement from the French authorities to deliver samples for scientific research (number AC-2008-812). The samples come from care and are requalified for research. The project was approved by the Institut Bergonié ethics committee (scientific advisory board). Every case was histologically reviewed by the pathologist subgroup from the French Sarcoma Group and classified according to the 2013 WHO classification by histology, IHC, and molecular genetics and cytogenetics when needed.

### Sample description

The screened series was composed of 112 sarcomas with complex genomics and five cell lines (CL; CL1 derived from an undifferentiated pleomorphic sarcoma T1; CL2 derived from a dedifferentiated liposarcoma; CL3 derived from a myxofibrosarcoma; and CL4 and CL5 derived from two leiomyosarcomas) for the first cohort.

The second and the third cohorts are composed of 27 synovial sarcomas and 74 GIST, respectively. All tumors have been histologically reviewed by a pathologist panel from the French Sarcoma Group.

### Cell line establishment and culture

Cell line establishment was performed as described previously (17). Authentication of cell line is analyzed by aCGH by comparing the cell line with the corresponding tumor origin.

The culture medium was composed of RPMI1640 with GlutaMAX (Gibco BRL, Life Technologies) supplemented with 10% FCS and 1% antibiotics (penicillin/streptomycin, Gibco BRL, Life Technologies). All cell lines were tested for mycoplasma by PCR (Sigma; LookOut Mycoplasma PCR Detection Kit) according to the manufacturer's recommendations.

### RNA extraction, sample preparation, and RNA-seq

RNA extraction from frozen and formalin-fixed paraffin-embedded (FFPE) samples, sample preparation, and RNA-seq were performed as described previously (18).

### Bioinformatics pipeline for fusion detection and gene expression

Bioinformatics analysis was performed as described previously (18).

Briefly, deFuse (v0.6.1; ref. 19) was used on curated FastQ files with ENSEMBL GRCh37.74 annotations. We kept candidate fusions with the following criteria: probability >50%, non-read-through, non-read-through like (same chromosome, indicated as deletion, coding/coding gene region, and genomic distance <20,000) and breakpoint homology <30.

TopHat-Fusion (v2.1.0; ref. 20) was used on curated FastQ files with the same annotations as described by Lesluyes et al. in 2016 (18). Fusion minimum distance was set to 10,000, and fusion anchor length was set to 13. Other parameters were similar to the expression processing.

ChimeraScan (v0.4.5; ref. 21) algorithm was used on raw FastQ files (equal-length reads restriction) with UCSC (fixed on 2016/02/09) annotations. Multiple hits parameter was set to 50. We kept fusions with the following criteria: non-read-through, score >5, spanning reads >2, and non-HLA/HLA fusions (due to sequence homology).

For the three detection algorithms, duplicated entries (same genes) and non-ORF conservation fusions were discarded.

Unsupervised clustering method was performed with Wald algorithm and Euclidean distance available in the *cluster* R package (v2.0.3). Differential gene expression analysis was performed with *DESeq2* R package (1.8.1; ref. 22). Gene interaction was performed using BioGRID (23). Gene Set Enrichment Analysis (GSEA; v2.2.0; refs. 24, 25) was used with Hallmarks gene sets from MSigDB (v5.0), gene set permutation type, RefSeq chip platform without gene symbol collapse, and a minimum set size of 10. Differentially exonic expression was performed by DEXSeq (6 vs. 40; ref. 26).

### RT-PCR and Sanger sequencing

Total RNA was reverse transcribed using High-Capacity cDNA Reverse Transcription Kit (Applied Biosystems) according to the manufacturer's instructions.

For PCR, primers were designed using Primer3 program (http://frodo.wi.mit.edu/primer3/) and are presented in Supplementary Table S1. Touchdown 60°C program has been used (TD 60°C; two cycles at 60°C, followed by two cycles at 59°C, two cycles at 58°C, three cycles at 57°C, three cycles at 56°C, four cycles at 55°C, four cycles at 54°C, five cycles at 53°C, and finally 10 cycles at 52°C). PCR was performed on 50 ng of cDNA using AmpliTaqGold DNA

Polymerase (Applied Biosystems). PCR products were then purified using ExoSAP-IT PCR Purification Kit (GE Healthcare), and sequencing reactions were performed with the Big Dye Terminator V1.1 Kit (Applied Biosystems) according to the manufacturer's recommendations. Samples were then purified using the Big Dye XTerminator Purification Kit (Applied Biosystems) according to the manufacturer's instructions, and sequencing was performed on a 3130xl Genetic Analyzer (Applied Biosystems). Sequence analysis was performed with SeqScape software v2.5 (Applied Biosystems).

### Quantitative RT-PCR

Expression of different *TRIO-TERT* and *TRIO* transcripts was studied with probes and primers listed in Supplementary Table S2. Normalization of expression was carried out with two reference genes: *ACTB* and *RPLP0*. Probes and primers (TaqMan Gene Expression Assay, Life Technologies) of these genes are Hs99999903_m1 and Hs99999902_m1, respectively. Reaction was performed with TaqMan Universal PCR Master Mix (Life Technologies) using StepOnePlus (Life Technologies) according to the manufacturer's recommendations. Expression was calculated with the formula: $\Delta C_t = C_{t_{TRIO-TERT}} - C_{t_{\text{reference gene}}}$ (27). Subsequently, difference of expression between both transcripts was calculated with the formula $2^{\Delta C_{t\,\text{transcript 1}-\text{transcript 2}}}$.

### FISH

FISH assay on FFPE cases T1, S867, and S909 was performed using the Histology FISH Accessory Kit (Dako) as described previously (28) on a 4-μm paraffin-embedded section. Regarding metaphase chromosome spreading on CL1, cells were incubated with colchicine overnight and resuspended in isotonic KCl buffer. Cells were finally fixed in standard 3:1 methanol:acetic acid final fixative. After several washes, cells were spread on a glass slide. Denaturation (5 minutes at 82°C for paraffin-embedded tissues and 1 minute at 73°C for chromosome spreading) and hybridization (overnight at 37°C) were achieved by placing the slides into a hybridizer (Dako). For the identification of the *TRIO* fusion, one BAC clone covering 5′ part of *TRIO* (RP11-1134M22; red signal) and two BAC clones covering 3′ part of *TRIO* (RP11-81P9, RP11-1079G4; green signals) were used; green and red fluorescent signals were analyzed in tumors using a Nikon Eclipse 80i fluorescence microscope with appropriate filters. Pictures were captured using a Hamamatsu C4742-95 CCD camera and analyzed with the Genikon software. A *TRIO* rearrangement was detected when red and green signals were separated in the nucleus. A *TRIO* rearrangement was considered as present if at least 10% of tumor cells showed a rearrangement pattern. Unbalanced rearrangements (fusion signal associated with at least one supernumerary red signal) are considered as positive case when chimeric transcript has been validated by RT-PCR and Sanger sequencing and with at least 10% rearranged signals.

### Affymetrix CytoScan HD Array

Genomic DNA was isolated using a standard phenol–chloroform extraction protocol. Affymetrix CytoScan HD Array (Affymetrix) was used according to the manufacturer's instructions. The test was conducted on DNA samples from *TRIO* translocated cases. CEL files obtained by scanning the CytoScan arrays were analyzed using the Chromosome Analysis Suite software (Affymetrix) and the annotations of the genome version GRCH37 (hg19).

### Immunofluorescence

Tissues were deparaffinized in xylene and rehydrated in a series of ethanol baths. For antigen retrieval, slides were incubated in DAKO Target Retrieval Solution, pH 9 (DAKO), for 20 minutes in a microwave oven. The primary antibodies and dilutions (dilution in DAKO REAL antibody diluent, DAKO) used in this study are as follows: anti-PML (PG-M3, 1:200, sc-966, Santa Cruz Biotechnology) and anti-TERF2 antibody (1:200, HPA001907, Sigma). All primary antibodies were incubated for 1 hour at room temperature. Secondary antibodies and dilutions used are as follows: anti-mouse immunoglobulins/FITC (1/400, Dako) and anti-rabbit IgG (H+L) Alexa Fluor 594 conjugate (1/500, Invitrogen). Slides were mounted with VECTASHIELD/DAPI medium (Vector Laboratories) and were then analyzed using a Nikon Eclipse 80i fluorescent microscope with appropriate filters. Pictures were captured using a Hamamatsu C4742-95 CCD camera.

### Design and infection of *TRIO-TERT* shRNA

Short hairpin RNA (shRNA) sequences targeting $TRIO_{33}$-$TERT_2$ and a nontargeting control sequence (Supplementary Table S3) were cloned into the doxycycline-inducible pLKO.1-neo lentiviral shRNA vector (Addgene). VSV-G–pseudotyped lentiviral particles were produced by cotransfection of 293T cells with pLKO.1 constructs and the compatible packaging plasmids psPAX2 and pVSVg. Cell lines were incubated overnight with lentiviral supernatants in the presence of 8 μg/mL polybrene (Sigma H9268), and stably transduced cells were selected with neomycin (0.1–1 mg/mL, Sigma 4727894001) for 10 days. Downregulation of $TRIO_{33}$-$TERT_{2/3}$ mRNA expression was controlled by qRT-PCR.

### Proliferation assay

Proliferation measurement was performed using the IncuCyte Live Cell Imaging System (Essen BioScience). CL1s were seeded at 3,000 cells per well in a 96-well plate with eight replicates for each conditions. Cells were pretreated with or without doxycycline (1 μg/mL, Sigma D3072) for 48 hours before proliferation analysis. Treatment was maintained during 5 days of experiment. Proliferation was monitored according to the manufacturer's recommendations (two pictures every 2 hours for each well).

### Data access

RNA-seq raw files (FastQ) are available on Sequence Read Archive under the accession numbers SRP057793 (contains 112 tumors) and SRP059536 (contains the five sarcoma cell lines: CL1 is M965, CL2 is M969, CL3 is M961, CL4 is M963, and CL5 is M964).

Expression data for the 117 samples are available on Gene Expression Omnibus under accession number GSE75885.

## Results

### RNA-seq analysis and fusion prediction

To identify fusion transcripts, we performed RNA-seq on 112 sarcomas with complex genetics (Table 1) and 5 sarcomas cell lines. Means of 78.34 (± 18.71) and 74.97 (± 17.83) million reads per sample were obtained after library sequencing following low quality 5′ and 3′ trims and overlap correction, respectively. DeFuse (19) analysis predicted a total of 10,382 fusion transcripts for all samples with a fusion mean of 88.74 (± 52.7) per sample

**Table 1.** Nontranslocation-related sarcomas cohort description ($N = 112$)

| Characteristics | Cohort ($N = 112$) |
|---|---|
| Median follow-up (years) | 2.94 (95% CI, 2.11–3.77) |
| Median age (years) | 64.5 (95% CI, 62–67) |
| Sex | |
| Female | 56 (50%) |
| Male | 56 (50%) |
| FNCLCC grade (%) | |
| 1 | 3 (2.68%) |
| 2 | 29 (25.89%) |
| 3 | 76 (67.86%) |
| Unknown | 4 (3.57%) |
| Histologic type (%) | |
| UPS | 36 (32.14%) |
| LMS | 33 (29.46%) |
| DDLPS | 18 (16.07%) |
| MFS | 15 (13.39%) |
| PLPS | 4 (3.57%) |
| PRMS | 4 (3.57%) |
| Other | 2 (1.79%) |
| Location | |
| Lower limb | 45 (40.18%) |
| Internal trunk | 25 (22.32%) |
| Trunk wall | 18 (16.07%) |
| Upper limb | 16 (14.29%) |
| GI tract | 3 (2.68%) |
| Gynecologic area | 3 (2.68%) |
| Head and neck | 2 (1.79%) |
| Relapse events (%) | |
| Metastasis | 38 (33.93%) |
| Local recurrences | 34 (30.36%) |
| Median size of tumor (mm; $n = 109$) | 100 (95% CI, 80–100) |

Abbreviations: CI, confidence interval; DDLPS, dedifferentiated liposarcoma; FNCLCC, *Fédération Française des Centres de Lutte Contre le Cancer*; GI, gastrointestinal; LMS, leiomyosarcoma; MFS, myxofibrosarcoma; PLPS, pleomorphic liposarcoma; PRMS, pleomorphic rhabdomyosarcoma; UPS, undifferentiated pleomorphic sarcoma.

(Fig. 1). Among them, 3,610 detected chimeric transcripts were actually read-throughs (chimeric transcripts between two adjacent genes and induced by transcription; ref. 29) according to deFuse and were consequently discarded from further processing. Following this selection, 6,772 potential fusion transcripts were kept. To identify in-frame fusion transcripts, we filtered this selection and focused on the 420 in-frame predicted fusions with conserved open reading frame (ORF) for each partner. Among these transcripts, eight presented a potential recurrence: *CTSC-RAB38* (13 samples), *GSE1-RP11-680G10.1* (12 samples), *NSUN4-FAAH* (8 samples), *CTBS-GNG5P2* (8 samples), *TRIO-TERT* (4 samples), *FARSA-SYCE2* (2 samples), *RPL11-TCEB3* (2 samples), and *TFG-GPR128* (2 samples). Among these eight transcripts, five are known to be read-throughs but evaded the deFuse filter: *CTSC-RAB38* and *TFG-GPR128* have been reported as read-throughs (30, 31), whereas *CTBS-GNG5P2*, *RPL11-TCEB3*, and *NSUN4-FAAH* are referenced in the ConjoinG database (32), which contains detailed information about identified read-throughs in the human transcriptome. *FARSA-SYCE2* and *GSE1-RP11-680G10.1* fusions have been identified in normal human tissues (RT-PCR and Sanger sequencing; Supplementary Fig. S1) and the two genes implicated in the fusion are on the same chromosome and transcribed on the same genomic strand. As they share similar characteristics as read-throughs, we discarded them from further analysis. The last potential in-frame recurrent chimeric transcript predicted by deFuse, $TRIO_{33/34}$-$TERT_{2/3}$ (fusion between *TRIO* either exon 33 or 34 and either *TERT* exon 2 or 3), occurred in four samples (CL1, S867, S829, and S822) and has not been detected in normal tissues (Fig. 2A and B). In addition, *TRIO-TERT* gene fusion has been validated by RT-PCR and Sanger sequencing in T1, the primary tumor of CL1 (Fig. 2A). No reciprocal transcript has been detected for these fusions (data not shown). Same

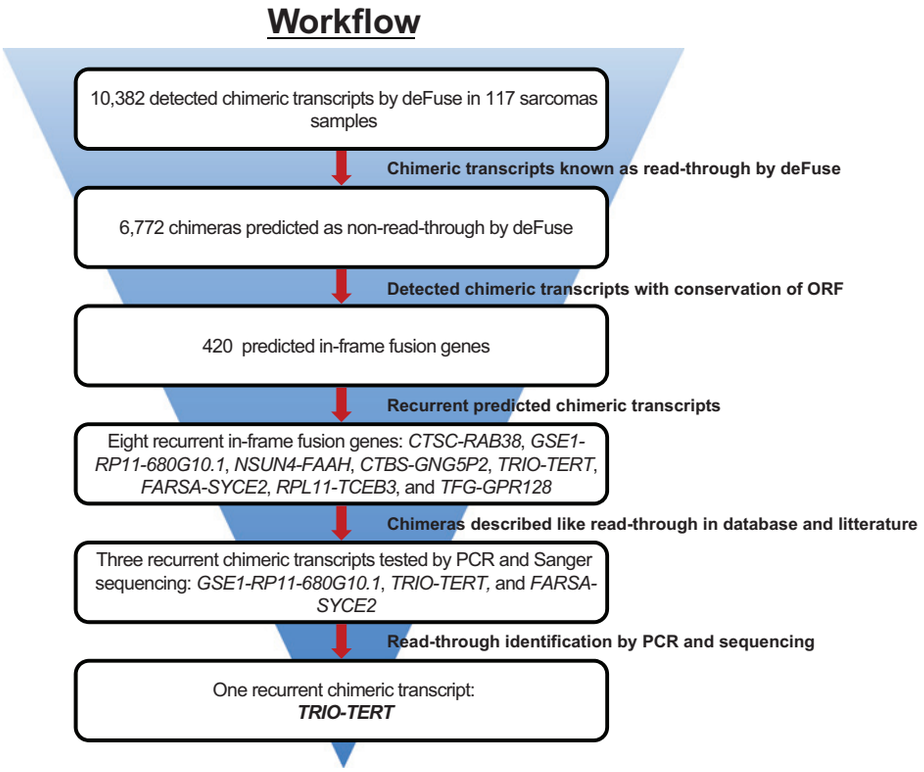


**Figure 1.**
Candidate fusion gene selection.

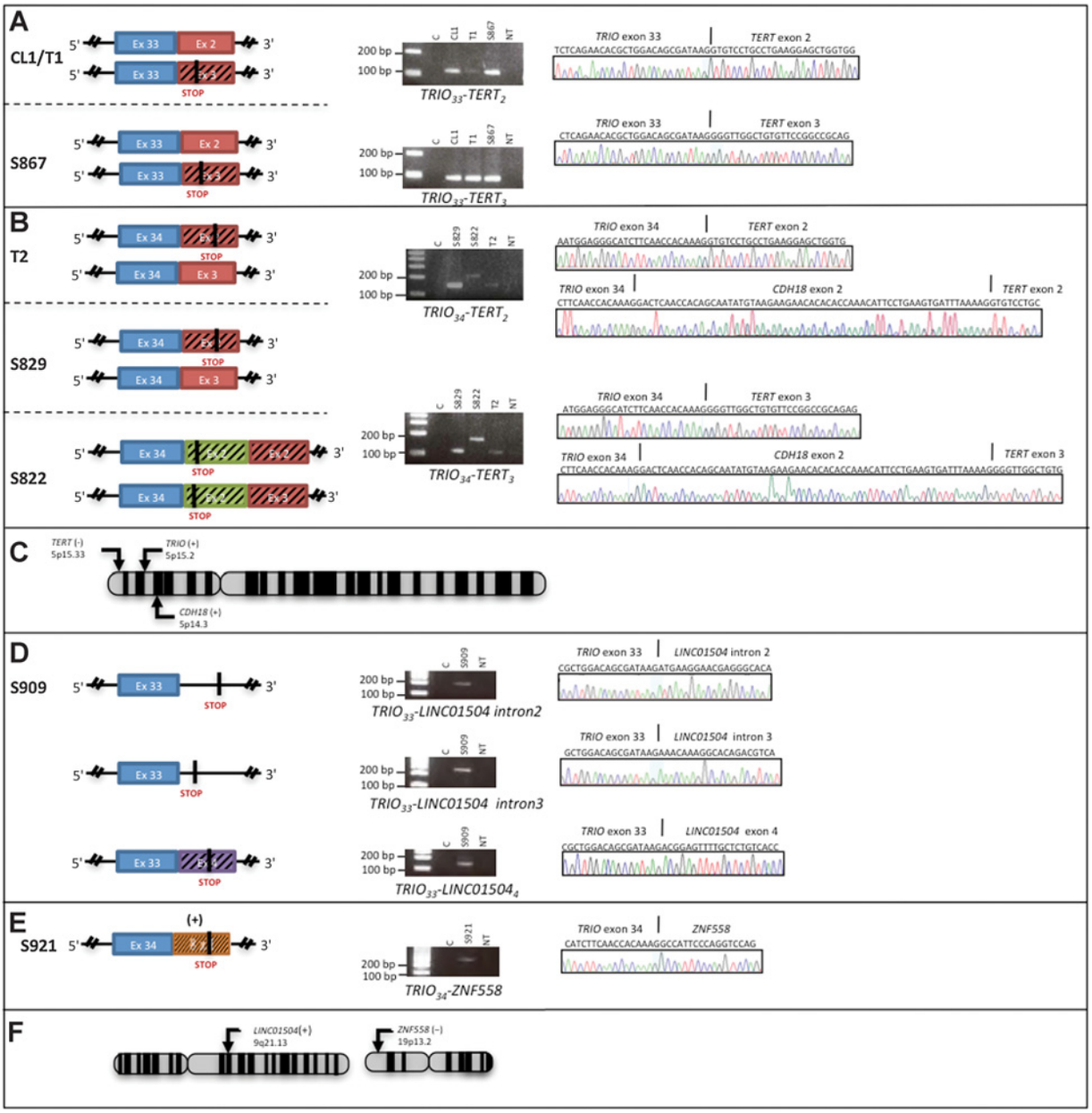


**Figure 2.**

Identification of seven fused *TRIO* cases. RT-PCR and chromatograms obtained with the four exon combinations involving *TRIO, TERT, LINC01504*, and *ZNF558* genes. **A** and **B,** Cases with $TRIO_{33}$-$TERT_{2/3}$ (**A**), $TRIO_{34}$-$TERT_{2/3}$, $TRIO_{34}$-CDH18-$TERT_{2/3}$ (**B**) expressions. **C,** Genomic location of *TRIO, TERT*, and *CDH18*. **D** and **E,** $TRIO_{33}$-*LINC01504* (**D**) and $TRIO_{34}$-*ZNF558* (**E**) expressions. **F,** Genomic location of *LINC01504* and *ZNF558*. **C,** PCR control; NT, normal tissue; *bp*, base pairs. Vertical black lines above chromatograms indicate sequence fusion between the two genes. All chimeric transcripts are represented by scheme for each case. Out-of-frame exons are indicated by black hatches. New STOP codons are indicated by a vertical black line on the scheme. *TRIO, TERT, CDH18, ZNF558*, and *LINC01504* exons are indicated in blue, red, green, orange, and purple respectively. + and − symbols (brackets), genomic strands.

analyses have been performed with two supplementary algorithms, TopHat-Fusion (20) and ChimerScan (21). *TRIO-TERT* is also the only recurrent in-frame chimeric transcript detected with these algorithms.

Consequently, *TRIO-TERT* fusion is the only recurring in-frame fusion identified in this cohort.

**What is the genomic alteration that results in the *TRIO-TERT* fusion transcript?**

aCGH analysis of three translocated cases (T1, S829, and S822) with high quality DNA available demonstrated that the *TRIO* (5p15.2) and *TERT* (5p15.33) loci (Fig. 2C) were rearranged (gain and/or amplification) in two of three cases (e.g., presented in

Supplementary Fig. S2A and S2B). Interestingly, in the *TRIO* gene, the copy number variation break is located in the region of fusion. We therefore hypothesized that the frequently observed chromosome 5p/*TRIO* amplification in sarcomas (11) could be associated, at least in some cases, to *TRIO* rearrangements. We thus reexamined the genomic profile of the 112 sarcomas tumors of RNA-seq cohort and 24 supplementary cases of nontranslocation-related sarcomas (Supplementary Table S4). Three cases presented a comparable *TRIO* amplification profile (T2, S909, and S921). Specifically, in T2, $TRIO_{34}$-$TERT_3$ fusion was detected by RT-PCR and Sanger sequencing (Fig. 2B). The two new remaining cases with *TRIO* amplification did not express *TRIO-TERT* gene fusion. We performed RNA-seq on these two additional samples, and deFuse analysis indicated that they both expressed a fusion gene involving *TRIO*, but not *TERT*. In sample S909, $TRIO_{33}$ is fused to *LINC01504*, and in sample S921, $TRIO_{34}$ is fused to *ZNF558*; both were subsequently validated by RT-PCR and Sanger sequencing (Fig. 2D–F).

To validate the genomic origin of the fusion, we performed FISH analysis in four cases with available and good enough quality FFPE blocks. A break-apart approach targeting *TRIO* validated rearrangement in the three interpretable cases (CL1/T1, S867, and S909) with 84%, 36%, and 58% of positive cells, respectively (Fig. 3).

### Analysis of *TRIO* fusion isoforms

In all cases, regardless of the partner, either *TRIO* exon 33 or exon 34 is fused. In five cases, fusion joined either *TRIO* exon 33 ($TRIO_{33}$-*TERT*: T1 and S867) or exon 34 ($TRIO_{34}$-*TERT*: cases S829, S822, and T2) to *TERT*, an exception being case S822, in which *CDH18* exon 2 is inserted in between *TRIO* exon 34 and *TERT*. Whatever the *TRIO* (or *CDH18* for case S822) exon, fusions occurs either with *TERT* exon 2 or exon 3 (*TRIO*-$TERT_2$ or *TRIO*-$TERT_3$).

As it has been reported that *TERT* exon 2 is subjected to alternative splicing (33), the expression of both isoforms should be due to alternative splicing instead of two translocation events (a much rarer genomic event).

Among these six distinct chimeric transcripts of the *TRIO-TERT* fusion, four ($TRIO_{33}$-$TERT_3$, $TRIO_{34}$-$TERT_2$, $TRIO_{34}$-$CDH18_2$-$TERT_2$, and $TRIO_{34}$-$CDH18_2$-$TERT_3$) did not conserve the *TERT* ORF with a stop codon after the last fused *TRIO* exon at 77, 353, 23, and 23 bp, respectively (Fig. 2A and B).

Given that all cases expressed both isoforms ($TRIO_{33/34}$-$TERT_2$ and $TRIO_{33/34}$-$TERT_3$), we sought to determine which isoform is preferentially expressed. Isoform-specific quantitative RT-PCR analysis showed that chimeric transcripts with *TERT* exon 3 were at least 15 times more expressed regardless the *TERT* ORF conservation (Supplementary Fig. S3).

In case S909, *TRIO* exon 33 is fused to *LINC01504*, leading to the expression of three isoforms: $TRIO_{33}$-$LINC01504_{intron2}$, $TRIO_{33}$-$LINC01504_{intron3}$, or to $TRIO_{33}$-$LINC01504_4$, resulting in the loss of the ORF after the breakpoint with a stop codon after the last *TRIO* exon at 146, 84, and 113 bp, respectively (Fig. 2D). Different transcripts observed in S909 could be explained by alternative splicing mechanisms as sequences near the fusion break-points in *LINC01504* introns 2 and 3 are predicted to be splicing sequences by Human Splicing Finder (34) with 66.9% and 74% of consensus value, respectively (Supplementary Fig. S4).

In case S921, *TRIO* exon 34 is fused to *ZNF558* exon 8 ($TRIO_{34}$-*ZNF558*) but on the *ZNF558* opposite strand resulting in the nonconservation of ORF of *ZNF558* with a stop codon after the breakpoint at 287 bp (Fig. 2E).

Seven cases have been identified: five expressing two isoforms of *TRIO-TERT* and two others cases expressing *TRIO* gene fusion with out-of frame interchromosomal gene partner. For *TRIO-TERT* cases, the preferential expressed isoform is $TRIO_{33/34}$-$TERT_3$ and not the isoform with *TERT* ORF conservation. All these results indicated that *TRIO* gene fusion lead to the formation of truncated TRIO protein.

Unfortunately, we could not detect these fusion proteins by Western blot analysis of sarcoma cell line lysates, due to the lack of sensitivity/specificity of the TRIO antibody available that recognize these fusion proteins (data not shown).

### Are *TRIO* fusions specific to sarcomas with complex genetics?

The seven identified translocated cases belong to different histotypes: three undifferentiated pleomorphic sarcomas, two dedifferentiated liposarcomas, one pleomorphic rhabdomyosarcoma, and one myxofibrosarcoma. According to the *Fédération Française des Centres de Lutte Contre le Cancer* grading system, five of them were classified as grade 3 (T1, S867, S829, S822, and S909) and two as grade 2 tumors (T2 and S921). Three tumors presented a metastatic relapse and two presented a local recurrence (Table 2). These results indicate a trend toward tumor aggressiveness without reaching significance considering the number of cases.

Specificity of all *TRIO* chimeric transcripts has been tested on two independent cohorts of 74 GISTs and 24 synovial sarcomas by RT-PCR. None have been identified in these nonpleomorphic

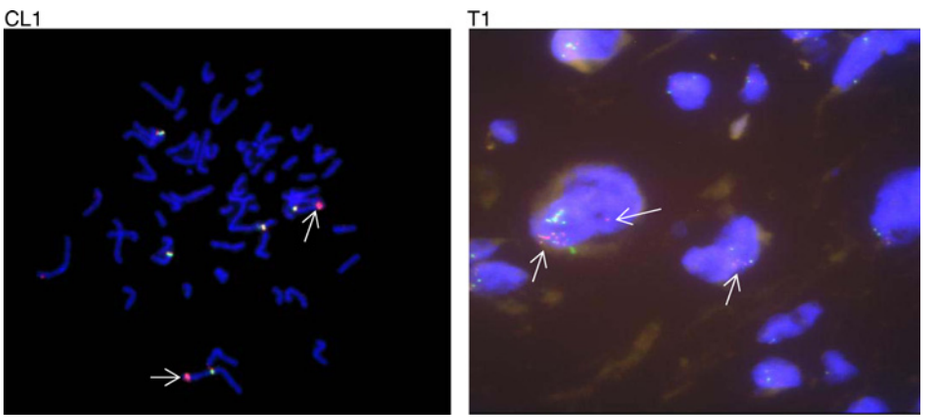


**Figure 3.**
FISH on one *TRIO* fusion gene case. On the representative picture of FISH, we could observe unbalanced rearrangement of *TRIO* highlighted by arrows in metaphase cell of CL1 and interphase cell of T1. BAC clone covering 5′ part of *TRIO* (red signal) and two BAC clones covering 3′ part of *TRIO* (green signals) were used.

**Table 2.** Clinical and pathologic data for individuals harboring *TRIO* gene fusion

| Case | Histotype | Grade | Location | Metastasis | Local recurrence | Genre | Chimeric transcripts | Chromosome gene 1 | Chromosome gene 2 | Break position gene 1 | Break position gene 2 | ORF conservation | New aa before stop codon |
|---|---|---|---|---|---|---|---|---|---|---|---|---|---|
| T1 | UPS | 3 | Trunk wall | Y | N | F | *TRIO*(ex33)-*TERT*(ex2) | 5 | 5 | 14406781 | 1294781 | Y | — |
| | | | | | | | *TRIO*(ex33)-*TERT*(ex3) | 5 | 5 | 14406781 | 1282739 | N | 24 |
| S867 | DD LPS | 3 | Lower limb | N | N | M | *TRIO*(ex33)-*TERT*(ex2) | 5 | 5 | 14406781 | 1294781 | Y | — |
| | | | | | | | *TRIO*(ex33)-*TERT*(ex3) | 5 | 5 | 14406781 | 1282739 | N | 24 |
| T2 | DD LPS | 2 | Extremities | N | N | M | *TRIO*(ex34)-*TERT*(ex2) | 5 | 5 | 14420130 | 1294781 | N | 117 |
| | | | | | | | *TRIO*(ex34)-*TERT*(ex3) | 5 | 5 | 14420130 | 1282739 | Y | — |
| S829 | PRMS | 3 | Lower limb | Y | Y | M | *TRIO*(ex34)-*TERT*(ex2) | 5 | 5 | 14420130 | 1294781 | N | 117 |
| | | | | | | | *TRIO*(ex34)-*TERT*(ex3) | 5 | 5 | 14420130 | 1282739 | Y | — |
| S822 | UPS | 3 | Upper limb | N | Y | M | *TRIO*(ex34)-*CDH18*(ex2)-*TERT* (ex2) | 5 | 5 | 14420130 | 1294781 | N | 7 |
| | | | | | | | *TRIO*(ex34)-*CDH18*(ex2)-*TERT* (ex3) | 5 | 5 | 14420130 | 1282739 | N | 7 |
| S909 | UPS | 3 | Internal trunk | Y | N | F | *TRIO*(ex33)-*LINC01504*(intron2) | 5 | 9 | 14406781 | 74939905 | N | 37 |
| | | | | | | | *TRIO*(ex33)-*LINC01504*(intron3) | 5 | 9 | 14406781 | 74948537 | N | 28 |
| | | | | | | | *TRIO*(ex33)-*LINC01504*(exon4) | 5 | 9 | 14406781 | 74950306 | N | 98 |
| S921 | MFS | 2 | Lower limb | N | N | F | *TRIO*(ex34)-*ZNF558* | 5 | 19 | 14420130 | 8932224 | N | 196 |

Abbreviations: aa: amino acid; DDLPS, dedifferentiated liposarcoma; F, female; M, male; MFS, myxofibrosarcoma; N, no; PRMS, pleomorphic rhabdomyosarcoma; UPS, undifferentiated pleomorphic sarcoma; Y, yes.

sarcoma cohorts associated to a specific oncogenic event (*KIT*/*PDGFRA* mutations and t(X;18) translocation, respectively; refs. 2–5).

*TRIO* gene fusion appears, thus, specific so far to nontranslocation-related sarcomas.

### Do *TRIO* fusions induce a specific transcriptomic program?

To test whether the presence of chimeric *TRIO* transcripts could be associated with a peculiar transcriptional profile of the fused *TRIO* samples (FTS), we applied unsupervised clustering method on 117 sarcomas with RNA-seq expression, including the six fused *TRIO* cases and the 111 nonfused *TRIO* samples (non-FTS; Supplementary Fig. S5). Our results indicate that FTSs do not have similar transcriptomic profiles as they did not cluster together. FTSs are localized within a subgroup of nonmuscular sarcomas, located in the extremities (adjusted Fisher $P = 0.014$ for both tumor differentiation and location).

We then performed a supervised differential gene expression analysis comparing fused and nonfused cases and identified 423 significant genes (Supplementary Fig. S6), out of which 69 were overexpressed in the FTS (Supplementary Table S5) and 354 overexpressed in non-FTS (Supplementary Table S6). We observed that *TRIO* and *TERT* were significantly more expressed (4.88 and 16.20 times, respectively) in FTS (adjusted Wald's $P = 4 \times 10^{-7}$ and $4.66 \times 10^{-3}$, respectively). To establish whether *TRIO* overexpression is due to wild-type or fused *TRIO*, we measured *TRIO* differential exonic expression of FTS versus non-FTS using DEXSeq (Supplementary Fig. S7; ref. 26). As the analysis could not be done on the whole non-FTS cohort ($n = 111$), we selected the 40 (maximum analysis capacity) samples that highly expressed *TRIO*. This analysis did not measure any differentially expressed exon in FTS versus non-FTS. However, we can see a slight exonic usage switch in layer "exon usage" starting at exon 34. Exons before this point are a bit more expressed in FTS, where *TRIO* expression is due to wild-type and fused *TRIO*. The trend is inversed after the breakpoint; exons 34 at 58 are a bit more expressed in non-FTS. In addition, this result shows that as no reciprocal fusions were observed in FTS and exons beyond 34 are expressed, wild-type *TRIO* is expressed in FTS. Genes interacting with *TRIO* and *TERT* were not identified as differentially expressed according to BioGRID (23).

GSEA (24, 25) was then applied on the Hallmarks new collection included in the MSidDB v5.0 database (containing 50 referenced gene sets). In fused *TRIO* samples, 16 significantly enriched gene sets were identified, mainly implicated in immunity/inflammation (6/16 gene sets), regulation of cell cycle (3/16), and cell proliferation and migration (3/16; Supplementary Fig. S8). Immunity gene set enrichment due to immune cell infiltration has been ruled out following a histologic review indicating that there was no significant difference between translocated and nontranslocated cases in terms of immune cell infiltration. In non-FTS, overexpressed gene sets are implicated, notably in myogenesis and adipogenesis (Supplementary Fig. S9).

These data suggest that *TRIO* fusion events are associated with overexpression of genes involved in immunity and inflammation, regulation of cell cycle, cell proliferation, and migration.

### Do fusions trigger TERT reactivation?

In a tumoral context, telomere length is maintained by two exclusive ways, either by telomerase reactivation or by the alternative lengthening of telomeres mechanism (ALT mechanism),

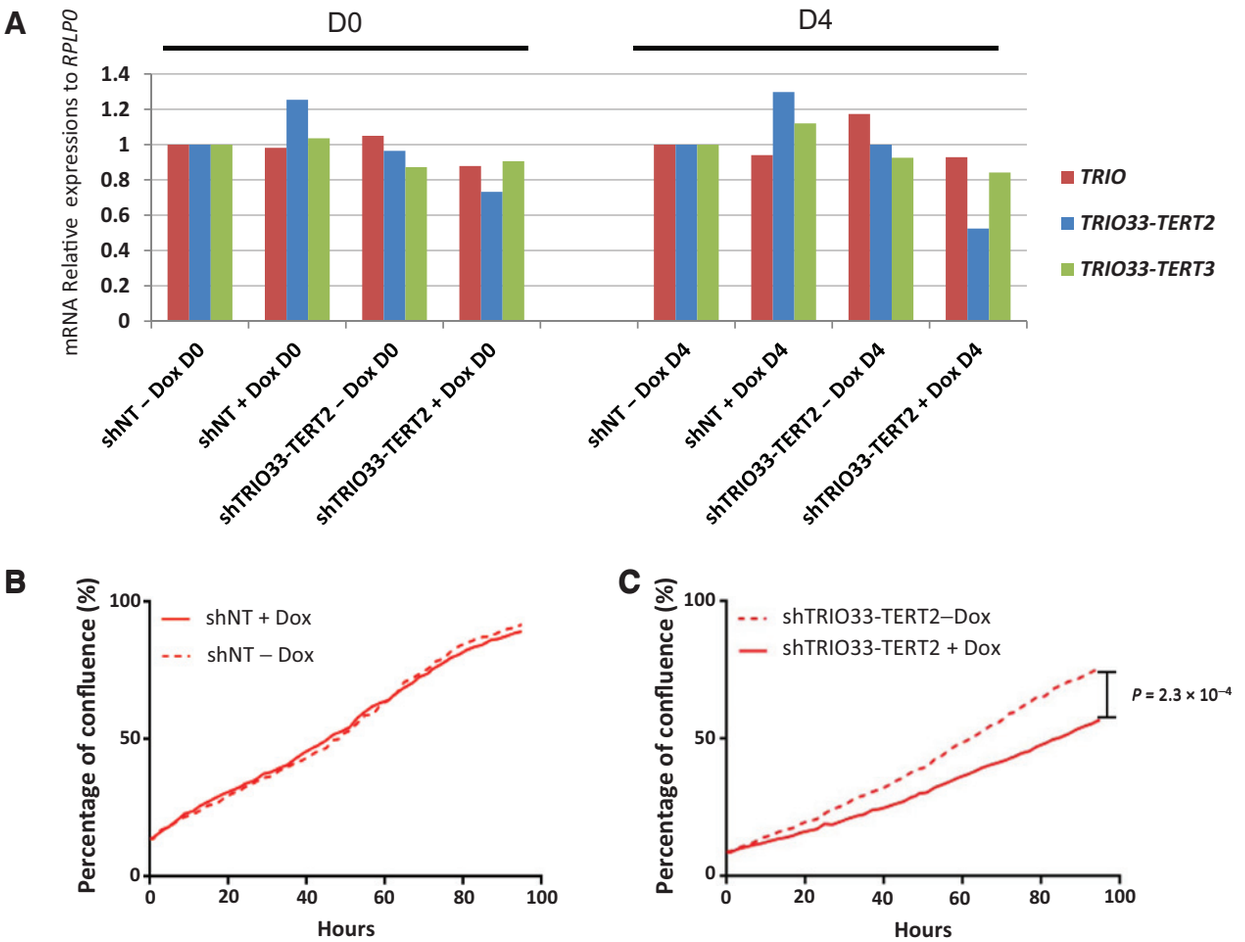


**Figure 4.**

Effect of *TRIO*$_{33}$-*TERT*$_2$ knockdown on cell proliferation. **A,** *TRIO*$_{33}$-*TERT*$_2$, *TRIO*$_{33}$-*TERT*$_3$, and *TRIO* mRNAs relative expression levels have been determined by qRT-PCR at day 0 (D0) and day 4 (D4) in the cell line expressing doxycycline-inducible shRNA-targeting *TRIO*$_{33}$-*TERT*$_2$ isoform (*shTRIO33-TERT2*) and the cell line expressing control shRNA (shNT, nontargeting shRNA). These cell lines have been treated (+) or not (−) with doxycycline (Dox) for 2 days before D0. ShNT–Dox is used as control. **B** and **C,** Proliferation assay has been performed during 4 days on CL1 with shRNA control (**B**) or sh*TRIO33-TERT2* (**C**) treated or not with doxycycline (representative of one experiment; $n = 2, 8$ replicates per condition). *P* values between sh*TRIO33-TERT2* – and + doxycycline conditions are significantly different (Wilcoxon's *P* with Benjamini–Hochberg adjustment < 0.05) from 27 hours of experiment. *P* value at 96 hours is indicated by the vertical line in graph.

and both mechanisms appear to be mutually exclusive (35, 36). In pleomorphic sarcomas, the ALT mechanism is very frequent (60% of cases; ref. 37). To test whether *TRIO-TERT* fusion could be associated with TERT reactivation, we evaluated the colocalization of PML and TERF2 as a hallmark of the ALT mechanisms, which, if negative, means that it is the telomerase reactivation pathway (38). The four *TRIO-TERT* interpretable cases were negative for PML/TERF2 colocalization and, consequently, negative for ALT mechanism. Moreover, S921 (*TRIO*$_{34}$-*ZNF558*) presented the same results and was also declared ALT negative (Supplementary Fig. S10).

### Do *TRIO* fusions trigger phenotype modifications?

To uncover the role of *TRIO* fusions, we performed *TRIO*$_{33}$-*TERT*$_{2/3}$ knockdowns in CL1 using lentivirally delivered shRNA contructs. Two shRNAs for each isoform were tested at day 0 and day 4 and only one allowed the specific decrease of *TRIO*$_{33}$-*TERT*$_2$ (50%) at 4 days without decreasing *TRIO* and *TRIO*$_{33}$-*TERT*$_3$ expressions (Fig. 4A). With respect to transcriptomic analysis, we thus used it to run proliferation assays in CL1. As shown in Fig. 4B and C, contrary to the nontargeting shRNA, knocking down *TRIO*$_{33}$-*TERT*$_2$ significantly reduces cell proliferation.

## Discussion

Sarcomas with complex genetics are tumors that harbor a high number of chromosomal rearrangements. To better understand the biology of these tumors, we searched for recurrent chimeric transcripts.

### Chimeric transcripts in nontranslocation-related sarcomas

In the current study, 10,382 potential chimeric transcripts have been predicted, and 3,604 of them were considered read-throughs by the detection algorithm deFuse. Although read-throughs were

not considered in this study, it has been reported that tumor-specific read-through expression could be involved in oncogenesis (39).

More than 80 filtered fusion transcripts were predicted per case in nontranslocation-related sarcomas, and most of the chimeric transcripts detected arose from intrachromosomal rearrangements and were not in-frame (96%). This is in agreement with data reported by Yoshihara and colleagues, regarding fusion transcript prediction in a large series of 4,366 cancers (various types excluding sarcomas; ref. 40). They showed that the high complexity of tumor genome is associated with a higher number of predicted fusion transcripts. Our results are consistent with the high genomic complexity levels of nontranslocation-related sarcomas. On the contrary, according to the data presented by Yoshihara and colleagues, approximately 36% of detected fusion transcripts were predicted to be in-frame in their cohort compared with 4.13% in our study. This suggests that chimeric transcripts could have other role(s) in nontranslocation-related sarcomas as they would mainly produce a truncated protein or no protein product at all.

### *TRIO* gene fusions lead to truncated TRIO protein expression

Here, we report recurrent *TRIO* fusions identified by RNA-seq and validated in 6 poorly differentiated pleomorphic sarcomas out of 117 (5.1%) and one dedifferentiated liposarcoma (T2) identified in aCGH analysis out of 26 nontranslocation-related sarcomas (3.8%). Three different *TRIO* fusion partners have been identified in this study, *TERT*, *LINC01504*, and *ZNF558*. Whatever the fusion partner, breakpoints in *TRIO* are consistently either after exons 33 or 34. This likely suggests that either these conserved domains, in the fused TRIO proteins, are essential or that genomic location of the breakpoint is specifically targeted by an unknown mechanism. Furthermore, two of the partners (*LINC01504* and *ZNF558*) are fused out-of-frame, suggesting that translocation leads to a truncated TRIO protein and that this truncated form is of a selective advantage for tumor cell. This hypothesis is strengthened by the isoform-specific quantitative analysis, showing that chimeric transcripts with an out-of-frame *TERT* fusion are the most expressed. It is even more strengthened by the differential expression analysis. For statistical consideration, GSEA (50 cancer Hallmarks) was applied instead of Gene Ontology (41) analysis, and we evidenced that *TRIO*-translocated cases significantly overexpressed genes involved in immunity/inflammation, cell proliferation, and migration.

TRIO protein has two GEF domains (42). While GEF1 mediates GDP to GTP exchange, leading to Rac1 and RhoG activation, GEF2 domain triggers RhoA activation. In addition to these domains, TRIO has a SEC14 domain, several spectrin repeats, two SH3 domains, an Ig-like domain, and a serine kinase domain. Unlike the GEF domains, the roles of these latter domains are still unclear. Rac1 and RhoG are members of Rho proteins controlling several pathways leading to cytoskeletal rearrangements, kinase activation, and gene transcription. They are implicated in cell proliferation and motility (43).

All *TRIO* fusions encode for TRIO N-terminal domains Sec14, spectrin, and GEF1 domain (Supplementary Fig. S11), which triggers Rac1 activation. Rac1 has been demonstrated to be directly involved in transformation and tumor progression (44). Rac1 acts by promoting anchorage-independent growth (45), proinflammatory pathway (46), proliferation, cell spreading, and migration by regulating lamellipodia formation (47, 48). Interestingly, *TRIO* gene fusions lead to the loss of the C-terminal GEF2, suggesting that the GEF2 domain is not associated to the process of tumor progression in sarcoma. This is consistent with the observation that most processes induced by TRIO depend on the activation of Rac1 by GEF1 and not on the activation of RhoA by GEF2 (49). Moreover, the depletion of $TRIO_{33}$-$TERT_2$ isoform demonstrates that *TRIO* fusion has an impact on cell proliferation. As this isoform is the least expressed in all cases, we hypothesize that the effect would be stronger if the $TRIO_{33}$-$TERT_3$ isoform was downregulated concomitantly (no shRNA available).

*TRIO* encodes at least seven different isoforms (49) and two of them (B and C), containing only the Sec14, spectrin, GEF1, and SH3 domains, are exclusively expressed in nervous system (50). Interestingly, the *TRIO* exons involved in the fusions (exons 1 to 33-34) are exactly the same as the ones observed in the two neuronal isoforms B and C, and as a consequence, they share the same protein domains. The role(s) of these two isoforms is unknown. Salhia and colleagues (51) have demonstrated that the transcriptional activation of the nervous system–specific *TRIO* isoform, through transfer in a different cellular context, could be an efficient way to hijack and remodel existing metabolic pathways for the benefit of tumor cells as demonstrated in glioblastoma (51).

### Telomerase reactivation in *TRIO*-fused cases

*TRIO* gene has been identified in fusion with three partners: *TERT*, *LINC01504*, and *ZNF558*. Although *TERT*'s role on elongation of telomeres is well known, the role of *LINC01504* and *ZNF558* is unknown. Stransky and colleagues (52) identified $TRIO_{33}$-$TERT_2$ fusion in two dedifferentiated liposarcomas. The authors suggest that this gene fusion could permit the expression of *TERT* in these tumors. In our study, the length of telomeres is maintained by telomerase reactivation and not by ALT mechanism in the *TRIO* gene fusions. *TERT* is overexpressed in these samples regardless of the *TRIO* fusion partner (i.e., *TERT*, *LINC01504*, and *ZNF558*), suggesting that, in these cases at least, telomerase activation is not associated with *TRIO* rearrangements. Moreover, in-frame *TERT* chimeric transcript loses the TEN domain of TERT permitting the fixation of *TR* RNA, the matrix for telomeres elongation (32). This prompts us to conclude that *TRIO-TERT* fusions do not trigger TERT reactivation in these tumors.

### *TRIO* gene fusion is specific to nontranslocation-related sarcomas

*TRIO* fusion transcripts have been detected exclusively in a cohort of sarcomas with complex genetics. We did not detect any *TRIO* chimeric transcript in large cohorts of GISTs and synovial sarcomas, which are both sarcoma subtypes associated with a specific genetic alteration and a very low genomic complexity. Moreover, in Yoshihara and colleagues' study (40), chimeric RNA-seq data of 4,366 tumor samples have been submitted to fusion detection, and *TRIO* fusion transcripts have not been detected in the whole cohort of various tumors (excluding sarcomas). *TRIO* fusions could therefore be quite specific to nontranslocation-related sarcomas, with an incidence of around 5%. It is the unique recurrent gene fusion so far identified in these aggressive nontranslocation-related sarcomas. Within this large sarcoma category, *TRIO* fusions are not limited to a specific histologic

subtype. This suggests that, unlike sarcomas with simple genetics and a recurrent specific translocation (e.g., Ewing sarcoma, synovial sarcoma, and alveolar rhabdomyosarcomas), which are associated to a specific transcriptomic profile (14), this chromosomal event is certainly not an initiating one but a secondary one caused by genetic instability of nontranslocation-related sarcomas and involved in tumor progression via cell proliferation enhancement. However, we did not have sufficient statistical evidence with seven cases to highlight this point, and we cannot exclude the possibility that more cases would permit to refine the biological and/or clinical context associated with these *TRIO* rearrangements.

## Disclosure of Potential Conflicts of Interest

No potential conflicts of interest were disclosed.

## Authors' Contributions

**Conception and design:** L. Lartigue, J.-M. Coindre, F. Chibon
**Development of methodology:** S. Schmidt, F. Chibon
**Acquisition of data (provided animals, acquired and managed patients, provided facilities, etc.):** L. Delespaul, T. Lesluyes, G. Pérot, J. Baud, P. Lagarde, S. Le Guellec, A. Neuville, P. Terrier, A. Debant, J.-M. Coindre, F. Chibon, D. Vince-Ranchère
**Analysis and interpretation of data (e.g., statistical analysis, biostatistics, computational analysis):** L. Delespaul, T. Lesluyes, G. Pérot, C. Brulard, L. Lartigue, J. Baud, J.-M. Coindre, F. Chibon
**Writing, review, and/or revision of the manuscript:** L. Delespaul, T. Lesluyes, L. Lartigue, S. Le Guellec, S. Schmidt, A. Debant, F. Chibon
**Study supervision:** F. Chibon

## Acknowledgments

Computer time for this study was provided by the computing facilities MCIA (Mésocentre de Calcul Intensif Aquitain) of the Université de Bordeaux and of the Université de Pau et des Pays de l'Adour. The authors thank Andreas Bikfalvi laboratory for granting access to IncuCyte. We are grateful to the people involved in the French Sarcoma Group (GSF) for clinical annotations and access to their samples: L. Guillou, F. Collin, A. Leroux, Y-M. Robin, M. C. Chateau, I. Peyrottes, and F. Mishellany. The authors would also like to thank Dr. Ravi Nookala of Institut Bergonié for the medical writing services.

## Grant Support

This work was supported by euroSARC (FP7-HEALTH-2011), Fondation ARC pour la recherche Contre le Cancer (to A. Debant), Ligue Contre le Cancer (Comité régional Gironde to F. Chibon and Comité régional Languedoc Roussillon to A. Debant) Inserm, and Integrated Cancer Research Site (SIRIC) of Bordeaux (BRIO-Bordeaux Oncology research).

The costs of publication of this article were defrayed in part by the payment of page charges. This article must therefore be hereby marked *advertisement* in accordance with 18 U.S.C. Section 1734 solely to indicate this fact.

Received February 2, 2016; revised June 27, 2016; accepted July 27, 2016; published OnlineFirst August 15, 2016.

## References

1. Fletcher CDM, Unni KK, Mertens F, editors. WHO Classification of Tumours of Soft Tissue and Bone. 4th ed. Lyon, France: IARC Press; 2013.
2. Nakahara M, Isozaki K, Hirota S, Miyagawa J, Hase-Sawada N, Taniguchi M, et al. A novel gain-of-function mutation of c-kit gene in gastrointestinal stromal tumors. Gastroenterology 1998;115:1090–5.
3. Delattre O, Zucman J, Melot T, Garau XS, Zucker JM, Lenoir GM, et al. The Ewing family of tumors–a subgroup of small-round-cell tumors defined by specific chimeric transcripts. N Engl J Med 1994;331:294–9.
4. Guillou L, Coindre J, Gallagher G, Terrier P, Gebhard S, de Saint Aubain Somerhausen N, et al. Detection of the synovial sarcoma translocation t (X;18) (SYT;SSX) in paraffin-embedded tissues using reverse transcriptase-polymerase chain reaction: a reliable and powerful diagnostic tool for pathologists. A molecular analysis of 221 mesenchymal tumors fixed in different fixatives. Hum Pathol 2001;32:105–12.
5. Sorensen PHB, Lynch JC, Qualman SJ, Tirabosco R, Lim JF, Maurer HM, et al. PAX3-FKHR and PAX7-FKHR gene fusions are prognostic indicators in alveolar rhabdomyosarcoma: a report from the children's oncology group. J Clin Oncol 2002;20:2672–9.
6. Chibon F, Mariani O, Derré J, Malinge S, Coindre JM, Guillou L, et al. A subgroup of malignant fibrous histiocytomas is associated with genetic changes similar to those of well-differentiated liposarcomas. Cancer Genet Cytogenet 2002;139:24–9.
7. Coindre J-M, Mariani O, Chibon F, Mairal A, De Saint Aubain Somerhausen N, Favre-Guillevin E, et al. Most malignant fibrous histiocytomas developed in the retroperitoneum are dedifferentiated liposarcomas: a review of 25 cases initially diagnosed as malignant fibrous histiocytoma. Mod Pathol 2003;16:256–62.
8. Chibon F, Mairal A, Fréneaux P, Terrier P, Coindre JM, Sastre X, et al. The RB1 gene is the target of chromosome 13 deletions in malignant fibrous histiocytoma. Cancer Res 2000;60:6339–45.
9. Pérot G, Chibon F, Montero A, Lagarde P, de Thé H, Terrier P, et al. Constant p53 pathway inactivation in a large series of soft tissue sarcomas with complex genetics. Am J Pathol 2010;177:2080–90.
10. Adamowicz M, Radlwimmer B, Rieker RJ, Mertens D, Schwarzbach M, Schraml P, et al. Frequent amplifications and abundant expression of TRIO, NKD2, and IRX2 in soft tissue sarcomas. Genes Chromosomes Cancer 2006;45:829–38.
11. Gibault L, Pérot G, Chibon F, Bonnin S, Lagarde P, Terrier P, et al. New insights in sarcoma oncogenesis: a comprehensive analysis of a large series of 160 soft tissue sarcomas with complex genomics. J Pathol 2011;223:64–71.
12. Chibon F, Mariani O, Mairal A, Derré J, Coindre J-M, Terrier P, et al. The use of clustering software for the classification of comparative genomic hybridization data. an analysis of 109 malignant fibrous histiocytomas. Cancer Genet Cytogenet 2003;141:75–8.
13. Mairal A, Chibon F, Rousselet A, Couturier J, Terrier P, Aurias A. Establishment of a human malignant fibrous histiocytoma cell line, COMA. Characterization by conventional cytogenetics, comparative genomic hybridization, and multiplex fluorescence *in situ* hybridization. Cancer Genet Cytogenet 2000;121:117–23.
14. Pierron G, Tirode F, Lucchesi C, Reynaud S, Ballet S, Cohen-Gogo S, et al. A new subtype of bone sarcoma defined by BCOR-CCNB3 gene fusion. Nat Genet 2012;44:461–6.
15. Chmielecki J, Crago AM, Rosenberg M, O'Connor R, Walker SR, Ambrogio L, et al. Whole-exome sequencing identifies a recurrent NAB2-STAT6 fusion in solitary fibrous tumors. Nat Genet 2013;45:131–2.
16. Robinson DR, Wu Y-M, Kalyana-Sundaram S, Cao X, Lonigro RJ, Sung Y-S, et al. Identification of recurrent NAB2-STAT6 gene fusions in solitary fibrous tumor by integrative sequencing. Nat Genet 2013;45:180–5.
17. Lagarde P, Brulard C, Pérot G, Mauduit O, Delespaul L, Neuville A, et al. Stable instability of sarcoma cell lines genome despite intra-tumoral heterogeneity: a genomic and transcriptomic study of sarcoma cell lines. Austin J Genet Genomic 2015;2:1014.
18. Lesluyes T, Pérot G, Largeau MR, Brulard C, Lagarde P, Dapremont V, et al. RNA sequencing validation of the Complexity Index in SARComas prognostic signature. Eur J Cancer 2016; 57:104–11.
19. McPherson A, Hormozdiari F, Zayed A, Giuliany R, Ha G, Sun MGF, et al. deFuse: an algorithm for gene fusion discovery in tumor RNA-Seq data. PLoS Comput Biol 2011;7:e1001138.
20. Kim D, Salzberg SL. TopHat-Fusion: an algorithm for discovery of novel fusion transcripts. Genome Biol 2011;12:R72.
21. Iyer MK, Chinnaiyan AM, Maher CA. ChimeraScan: a tool for identifying chimeric transcription in sequencing data. Bioinformatics 2011; 27:2903–4.
22. Love MI, Huber W, Anders S. Moderated estimation of fold change and dispersion for RNA-seq data with DESeq2. Genome Biol 2014; 15:550.

23. Chatr-Aryamontri A, Breitkreutz B-J, Oughtred R, Boucher L, Heinicke S, Chen D, et al. The BioGRID interaction database: 2015 update. Nucleic Acids Res 2015;43:D470–8.
24. Mootha VK, Lindgren CM, Eriksson K-F, Subramanian A, Sihag S, Lehar J, et al. PGC-1alpha-responsive genes involved in oxidative phosphorylation are coordinately downregulated in human diabetes. Nat Genet 2003; 34:267–73.
25. Subramanian A, Tamayo P, Mootha VK, Mukherjee S, Ebert BL, Gillette MA, et al. Gene set enrichment analysis: a knowledge-based approach for interpreting genome-wide expression profiles. Proc Natl Acad Sci USA 2005;102:15545–50.
26. Anders S, Reyes A, Huber W. Detecting differential usage of exons from RNA-seq data. Genome Res 2012;22:2008–17.
27. De Preter K, Speleman F, Combaret V, Lunec J, Laureys G, Eussen BHJ, et al. Quantification of MYCN, DDX1, and NAG gene copy number in neuroblastoma using a real-time quantitative PCR assay. Mod Pathol 2002; 15:159–66.
28. Terrier-Lacombe MJ, Guillou L, Chibon F, Gallagher G, Benhattar J, Terrier P, et al. Superficial primitive Ewing's sarcoma: a clinicopathologic and molecular cytogenetic analysis of 14 cases. Mod Pathol 2009;22:87–94.
29. Akiva P, Toporik A, Edelheit S, Peretz Y, Diber A, Shemesh R, et al. Transcription-mediated gene fusion in the human genome. Genome Res 2006;16:30–6.
30. Grosso AR, Leite AP, Carvalho S, Matos MR, Martins FB, Vítor AC, et al. Pervasive transcription read-through promotes aberrant expression of oncogenes and RNA chimeras in renal carcinoma. Elife 2015;4:pii: e09214.
31. Nacu S, Yuan W, Kan Z, Bhatt D, Rivers CS, Stinson J, et al. Deep RNA sequencing analysis of readthrough gene fusions in human prostate adenocarcinoma and reference samples. BMC Med Genomics 2011;4:11.
32. Prakash T, Sharma VK, Adati N, Ozawa R, Kumar N, Nishida Y, et al. Expression of conjoined genes: another mechanism for gene regulation in eukaryotes. PLoS One 2010;5:e13284.
33. Withers JB, Ashvetiya T, Beemon KL. Exclusion of exon 2 is a common mRNA splice variant of primate telomerase reverse transcriptases. PLoS One 2012;7:e48016.
34. Desmet F-O, Hamroun D, Lalande M, Collod-Béroud G, Claustres M, Béroud C. Human Splicing Finder: an online bioinformatics tool to predict splicing signals. Nucleic Acids Res 2009;37:e67.
35. Autexier C, Lue NF. The structure and function of telomerase reverse transcriptase. Ann Rev Biochem 2006;75:493–517.
36. Cesare AJ, Reddel RR. Alternative lengthening of telomeres: models, mechanisms and implications. Nat Rev Genet 2010;11:319–30.
37. Marzec P, Armenise C, Pérot G, Roumelioti F-M, Basyuk E, Gagos S, et al. Nuclear-receptor-mediated telomere insertion leads to genome instability in ALT cancers. Cell 2015;160:913–27.
38. Hu J, Hwang S-S, Liesa M, Gan B, Sahin E, Jaskelioff M, et al. Antitelomerase therapy provokes ALT and mitochondrial adaptive mechanisms in cancer. Cell 2012; 148:651–63.
39. Varley KE, Gertz J, Roberts BS, Davis NS, Bowling KM, Kirby MK, et al. Recurrent read-through fusion transcripts in breast cancer. Breast Cancer Res Treat 2014;146:287–97.
40. Yoshihara K, Wang Q, Torres-Garcia W, Zheng S, Vegesna R, Kim H, et al. The landscape and therapeutic relevance of cancer-associated transcript fusions. Oncogene 2015;34:4845–54.
41. Eden E, Navon R, Steinfeld I, Lipson D, Yakhini Z. GOrilla: a tool for discovery and visualization of enriched GO terms in ranked gene lists. BMC Bioinformatics 2009;10:48.
42. Debant A, Serra-Pagès C, Seipel K, O'Brien S, Tang M, Park SH, et al. The multidomain protein Trio binds the LAR transmembrane tyrosine phosphatase, contains a protein kinase domain, and has separate rac-specific and rho-specific guanine nucleotide exchange factor domains. Proc Natl Acad Sci USA 1996;93:5466–71.
43. Hall A. Rho GTPases and the actin cytoskeleton. Science 1998;279:509–14.
44. Jaffe AB, Hall A. Rho GTPases in transformation and metastasis. Adv Cancer Res 2002;84:57–80.
45. Seipel K, Medley QG, Kedersha NL, Zhang XA, O'Brien SP, Serra-Pages C, et al. Trio amino-terminal guanine nucleotide exchange factor domain expression promotes actin cytoskeleton reorganization, cell migration and anchorage-independent cell growth. J Cell Sci 1999;112:1825–34.
46. Van Rijssel J, Timmerman I, Van Alphen FPJ, Hoogenboezem M, Korchynskyi O, Geerts D, et al. The Rho-GEF Trio regulates a novel pro-inflammatory pathway through the transcription factor Ets2. Biol Open 2013; 2:569–79.
47. Vaqué JP, Dorsam RT, Feng X, Iglesias-Bartolome R, Forsthoefel DJ, Chen Q, et al. A genome-wide RNAi screen reveals a Trio-regulated Rho GTPase circuitry transducing mitogenic signals initiated by G protein-coupled receptors. Mol Cell 2013;49:94–108.
48. van Rijssel J, Hoogenboezem M, Wester L, Hordijk PL, Van Buul JD. The N-terminal DH-PH domain of Trio induces cell spreading and migration by regulating lamellipodia dynamics in a Rac1-dependent fashion. PLoS One 2012;7:e29912.
49. Schmidt S, Debant A. Function and regulation of the Rho guanine nucleotide exchange factor Trio. Small GTPases 2014;5:e29769.
50. Portales-Casamar E, Briançon-Marjollet A, Fromont S, Triboulet R, Debant A. Identification of novel neuronal isoforms of the Rho-GEF Trio. Biol Cell 2006;98:183–93.
51. Salhia B, Tran NL, Chan A, Wolf A, Nakada M, Rutka F, et al. The guanine nucleotide exchange factors trio, Ect2, and Vav3 mediate the invasive behavior of glioblastoma. Am J Pathol 2008;173:1828–38.
52. Stransky N, Cerami E, Schalm S, Kim JL, Lengauer C. The landscape of kinase fusions in cancer. Nat Commun 2014;5:4846.